

# Design and Analysis of a Three Phase Transformerless Hybrid Series Active Power Filter based on Sliding Mode Control Using PQ-theory And Stationary Reference Frames

Vinay Kumar Naguboina<sup>1</sup>, Satish Kumar Gudey<sup>1</sup>

**Abstract:** In this work, a Three phase Transformerless Hybrid Series Active Power Filter (THSeAF) based on Sliding Mode Control (SMC) is proposed to mitigate the voltage and current distortions present in an electrical distribution systems (EDS). A Sliding Mode Controller is designed by controlling the parameters present on the load side as well as source side of the system. Three separate voltage source converters (VSC) are used. The modelling of the system is derived by considering a single-phase system by using state space analysis. The frequency response characteristics have been derived for the single-phase system and the stability of the system is studied. It is observed that the system has good stability margins when the SMC is applied at the source side compared to load side. Simulation results obtained in PSCAD/EMTDC v4.6 have been observed for power quality issues like voltage sags, voltage swells, voltage distortions, voltage unbalances and their concurrent occurrence. The approach of stationary reference frame was used for source side control and PQ theory is used for load side control. It is observed that the proposed controller works well in obtaining a stable and constant load voltage during these power quality issues. The difference in settling time observed is around 4 ms for the load side and source side control. The THD present in the load voltage is near about 1%. The SMC is found to be robust in obtaining a constant load voltage with low THD and an improved power factor.

**Keywords:** Electrical Distribution System (EDS), Sliding Mode Control (SMC), Transformerless Hybrid series Active power Filter (THSeAF), Voltage Source Converter (VSC).

## 1 Introduction

Nowadays the usage of Power Electronics converters has been increased drastically. This has increased the non-linearity in grid current [1]. The increase

---

<sup>1</sup>Department of Electrical and Electronics Engineering, Gayatri Vidya Parishad College of Engineering (Autonomous), Visakhapatnam, Andhra Pradesh, India-530041;  
Emails: naguboina.vinay@gmail.com, satishgudey5@gvpce.ac.in

in non-linearity of grid current will adversely affect the system voltage. Sensitive or Linear loads are connected in parallel with the non-linear loads at the point of common coupling. Fig. 1a shows the block diagram representation of an Electrical Distribution system.

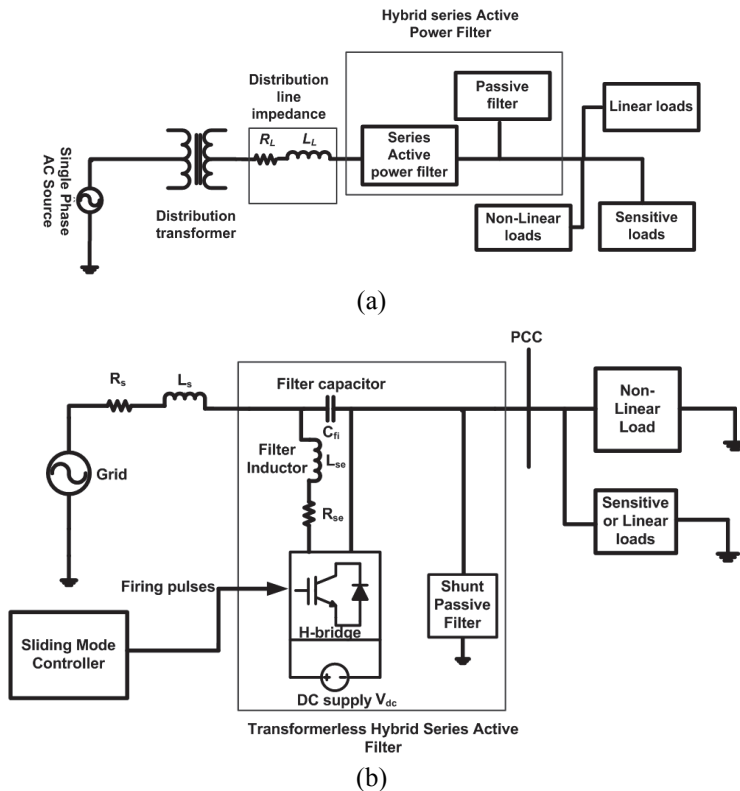


**Fig. 1** – (a) Block diagram of electrical distribution system;  
 (b) Transformerless Hybrid series Active Power Filter.

This non-linear current and non-linear voltage adversely affects these loads and hence their performance [2]. In order to protect these linear loads from the distortions, a compensating device has to be designed. There are various kinds of filters available to mitigate these unwanted distortions. Among them passive filters are used to mitigate the harmonics previously [3]. These filters mainly consist of various combinations of  $L$ ,  $C$  and  $R$  elements. Bulk, oversize and resonance effects are the drawbacks of using passive filters. To overcome these drawbacks, focus has been shifted towards Active Power Filters [4] which mainly consists of power electronic converters. These filters will inject or absorb power in such a way that the harmonic component will be zero. There are various kinds of Active Filters available like Series Active Power Filters,

Shunt Active Power Filters and Hybrid Active Power Filters [5]. There is a device which is known as Unified Power Quality Conditioner (UPQC) which consists of both Series Active Power Filter and Shunt Active Power Filter [6, 7]. The drawback observed using this device is the requirement of two separate controllers for Series Active Power Filter and Shunt Active Power Filter separately [8]. Nowadays research has been shifted towards the hybrid compensation which consists of combination of Active Power Filters and Passive filters. Among the available filters combination of Series Active Power Filters and Shunt Passive Filter as Hybrid active filters is chosen in this work. Fig. 1b represents the block diagram of Hybrid Series Active Power Filter. The Series Active Power Filter offers a high impedance path for the harmonics and low impedance path to the fundamental frequency components [9]. The Shunt Passive Filter is placed mainly to assist the operation of a Series Active Power Filter. It is tuned in such a way that it will create the low impedance path to the harmonic components and high impedance path to the fundamental frequency components [10]. The Series Active power filter has been tested individually with and without the Shunt Passive Filter. It has been observed that the requirement of DC Auxiliary supply is minimal if Series Active Power Filter is used in combination with Shunt Passive Filter. Hence Hybrid compensation is preferred when compared to the isolated mode [11].

## 2 Modeling of THSeAF using State Space Analysis

In the designed system the controller is implemented on the load side i.e. the reference signals are generated from the voltage across the shunt filter capacitor  $C$  and current through the filter capacitor  $i_c$ .

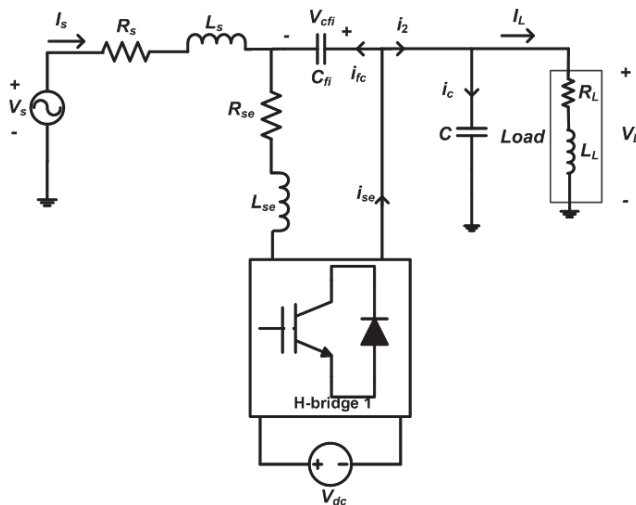


Fig. 2a – Equivalent circuit for THSeAF.

The state space model is derived using the equivalent circuit shown in Fig. 2a for THSeAF [12].  $C_{fi}$  represents the filter capacitor,  $L_{se}$  indicates the filter inductor and  $R_{se}$  indicates the damping resistor.

The dc link voltage  $V_{dc}$  is supported either by a grid connected rectifier or by energy storing elements like a battery.

$$\dot{X} = Ax + b_1u + b_2V_s + b_3i_L, \quad (1)$$

$$y = cx. \quad (2)$$

Few expressions derived using KVL and KCL are given in (3) and (4) for the circuit shown in Fig. 2a.

$$\left. \begin{aligned} i_c &= c \frac{dv_L}{dt} \\ \frac{dv_{c_{fi}}}{dt} &= \frac{i_{se}}{c_{fi}} - \frac{i_c}{c_{fi}} - \frac{i_L}{c_{fi}} \end{aligned} \right\} \quad (3)$$

$$\left. \begin{aligned} \frac{di_c}{dt} &= \frac{v_s}{L_s} - \frac{R_s}{L_s} i_c - \frac{R_s}{L_s} i_L + \frac{v_{c_{fi}}}{L_s} - \frac{v_L}{L_s} - \frac{v_L}{L_L} + \frac{i_L R_L}{L_L} \\ \frac{di_{se}}{dt} &= -\frac{v_{c_{fi}}}{L_{se}} - \frac{R_{se}}{L_{se}} + \frac{v_{dc}}{L_{se}} u \end{aligned} \right\} \quad (4)$$

$$\begin{bmatrix} \dot{v}_{c_{fi}} \\ \dot{v}_L \\ \dot{i}_c \\ \dot{i}_{se} \end{bmatrix} = \begin{bmatrix} 0 & 0 & -\frac{1}{C_{fi}} & \frac{1}{C_{fi}} \\ 0 & 0 & \frac{1}{C} & 0 \\ \frac{1}{L_s} & -\frac{1}{L_s} - \frac{1}{L_L} & -\frac{R_s}{L_s} & 0 \\ -\frac{1}{L_{se}} & 0 & 0 & -\frac{R_{se}}{L_{se}} \end{bmatrix} \begin{bmatrix} v_{c_{fi}} \\ v_L \\ i_c \\ i_{se} \end{bmatrix} + \quad (5)$$

$$+ \begin{bmatrix} 0 \\ 0 \\ 0 \\ \frac{V_{dc}}{L_{se}} \end{bmatrix} u + \begin{bmatrix} 0 \\ 0 \\ \frac{1}{L_s} \\ 0 \end{bmatrix} V_s + \begin{bmatrix} -\frac{1}{C_{fi}} \\ 0 \\ -\frac{R_s}{L_s} + \frac{R_L}{L_L} \\ 0 \end{bmatrix} i_L.$$

Four state variables ( $V_{cfi}$ ,  $V_L$ ,  $i_c$ ,  $i_{se}$ ) are chosen to derive the state space model from the equivalent circuit shown in Fig. 2a [13]. The stability of the system is analyzed using gain margins and phase margins obtained from the frequency response characteristic. Fig. 2b shows the frequency response characteristic of THSeAF using state feedback approach when the output matrix  $C = [0 \ 1 \ 1 \ 0]$ . The open loop transfer function is obtained using the expression  $G(s) = C(sI - A)^{-1}B$ . It is clear that the obtained system is a stable system with a gain margin of 74.1dB (should be infinity) and a phase margin of 87.5 degrees. Hence it can be concluded that low stability margins is obtained with the state variables ( $V_L$ ,  $i_c$ ) considered. If the state variables considered are  $v_{cfi}$ ,  $i_{se}$  the stability would be better compared to the load side control variables. It is discussed in Section 4.1. The model derived can well be used to find the frequency response characteristic with different control variables for analyzing the stability of the system.

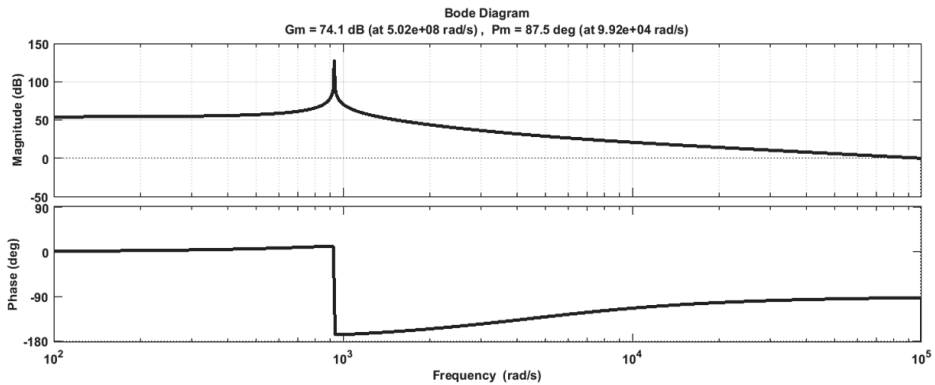


**Fig. 2b** – Frequency response characteristics of THSeAF with load side control.

## 2 Sliding Mode Controller

In this proposed work Sliding Mode Controller (SMC) is chosen as it is robust in nature. Sliding Mode Controller as the name indicates, forces the system response to slide over the desired response [14, 15]. It mainly depends upon the two parameters i.e. sliding surface and the sliding coefficients. Designing the sliding surface  $s_e$  helps in bringing the control variable  $x(t_0)$  to the sliding surface  $x(t_1)$  and then subsequently sliding on the surface to the ultimate origin O i.e. stable operating point. Proper selection of sliding coefficients helps in bringing the system response to settle at the desired response even during perturbations or disturbances within a desired time constant. The block diagram representation of a three-phase system considered for the simulation is shown in the Fig. 3b. The considered system consists of three SMC's which are used to

obtain a desired response during voltage sags, swells and unbalanced conditions. The voltage and current distortions present in each phase is analysed separately.

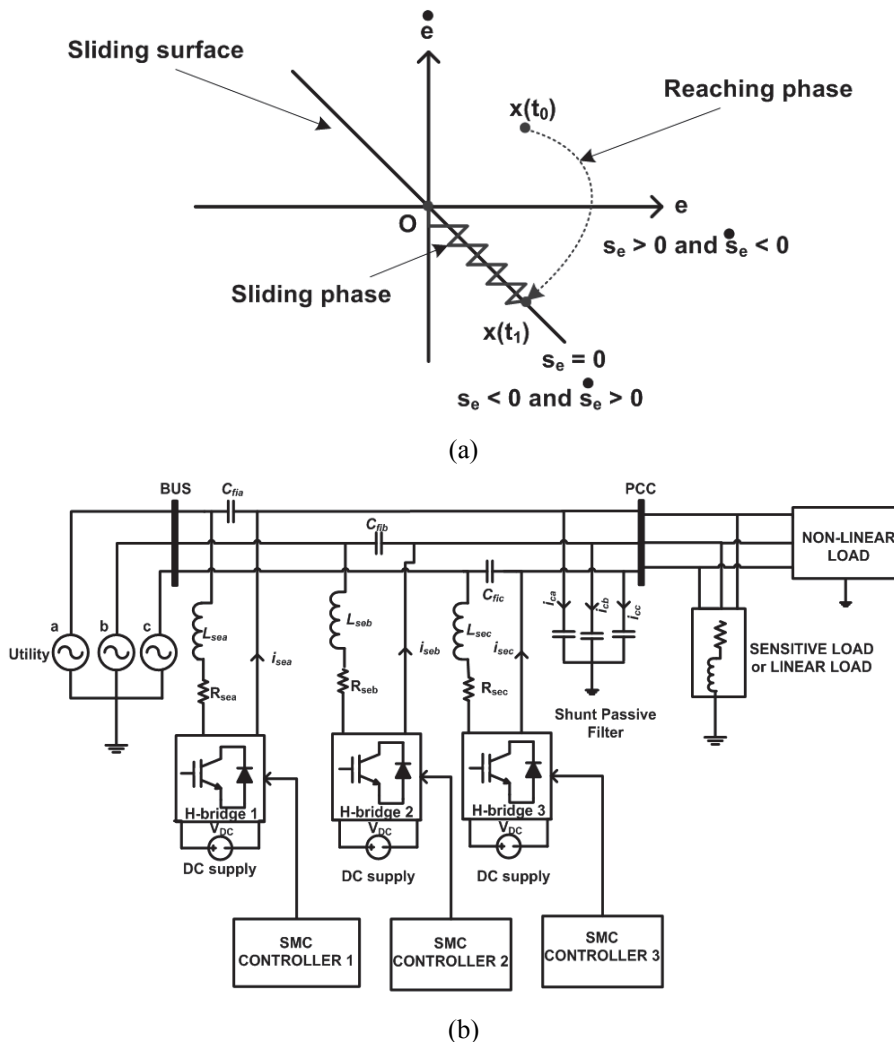


Fig. 3 – (a) Sliding surface of SMC; (b) Block diagram representation of three phase THSeAF with SMC's.

### 3 Load Side SMC Control Using Sine Wave Generators as References – Simulation Results and Discussions

The block diagram representation of the SMC controller used in a three-phase system is as shown in the Fig. 4.

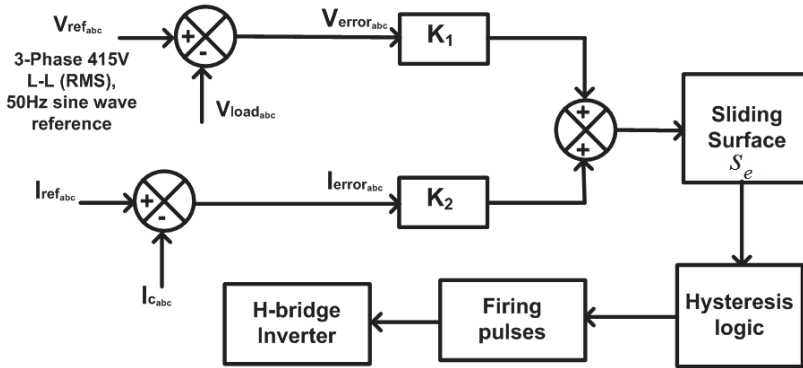


Fig. 4 – Block diagrammatic representation of SMC for a three-phase system.

The sliding surface used for the work is a linear one given by (6) [10]. The sliding coefficients  $k_1$  and  $k_2$  are taken as per the desired time constant.

$$s_e = k_1(V_{ref_{abc}} - V_{load_{abc}}) + k_2(I_{ref_{abc}} - I_{cap_{abc}}). \quad (6)$$

A THSeAF of rating 10kVA is considered for a three-phase system in this work. Linear and non-linear loads are connected at the point of common coupling. A shunt passive filter capacitance is selected based on the power factor improvement required at the load end. Using (7), the value of the capacitance  $C$  is calculated.  $Q_c, X_c$  and  $\phi_1, \phi_2$  are the reactive VARs required, capacitive reactance and initial and final phase angles for power factor correction.

$$\left. \begin{aligned} Q_c &= P(\tan \phi_1 - \tan \phi_2) \\ X_c &= \frac{V_s^2}{Q_c} \\ C &= \frac{(X_c)^{-1}}{\omega} \end{aligned} \right\}. \quad (7)$$

The configuration parameters considered for the simulation of three phase system is as shown in the **Table 1**.

A DC voltage source of 500 V is considered as it is sufficient to produce a pure sine wave in an inverter. The filter parameters  $L_{se}$  and  $C_{fi}$  are calculated for a 8 kW 0.8 lagging power factor system. A variable switching frequency operation using hysteresis logic is used in the proposed SMC.

**Table 1**  
Configuration Parameters.

Symbol	Definition	Value
THSeAF	Transformerless Hybrid Series Active Power Filter	10 kVA
$V_s$	Line phase-to-neutral voltage	339V (max)
$f$	System frequency	50Hz
$L_s$	line inductance	20 $\mu$ H
$R_s$	line resistance	0.5 $\Omega$
$R_{non}, L_{non}$	Non-linear Load (diode bridge rectifier)	11.5 $\Omega$ , 20mH
$P_L$	Linear load	7 kVA
$P_{non-lin}$	Non-Linear load	3.3-kVA
$L_{se}$	filter inductance	5mH
$C_{fi}$	filter capacitance	10 $\mu$ F
$R_{se}$	damping resistance	1 $\Omega$
$C$	Shunt passive filter Capacitance	228 $\mu$ F
$V_{dc}$	DC auxiliary power supply	500V
$pf$	Linear load power factor	0.8 lag
$K_1, K_2$	Sliding coefficients (tuned)	200, 1000

### 3.1 Voltage sag and voltage swell

In this simulation, balanced voltage sags have been created in three individual phases of the three-phase system. A voltage Sag of 20% for a period of time  $t=100$  ms was injected into the system and then the resultant output (phase to neutral) voltage and current through the linear loads has been checked. From Figs. 5a and 5b it is clear that the load voltages at PCC is controlled and maintained as sinusoidal even during sag occurrence in the source voltage. The load phase voltage and current of 240 V (rms), 10A (rms) is maintained.

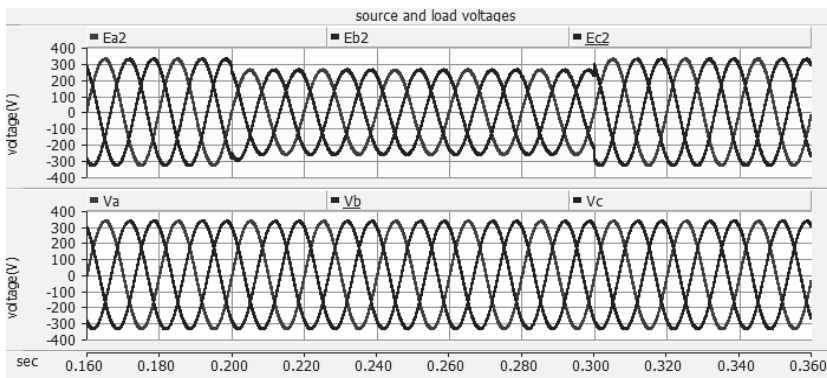


**Fig. 5a** – Three phase Grid voltages and Output (Phase to Neutral) voltages at load terminals for voltage sag.



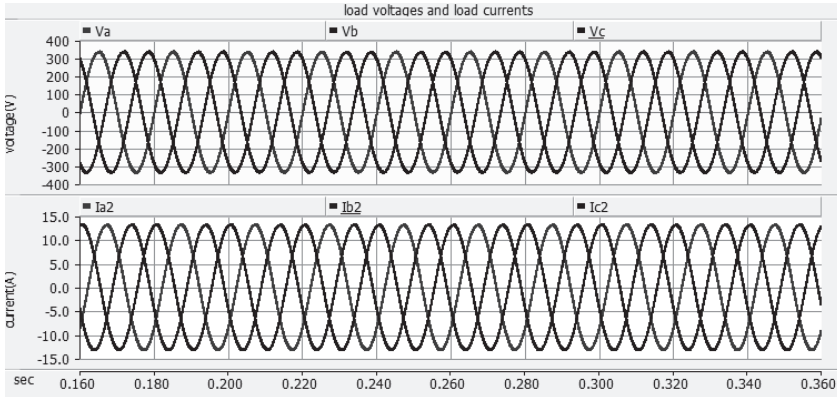


**Fig 5b** – Output (Phase to Neutral) voltages at load terminals and current through load terminals for voltage sag.

The power factor of the load is increased slightly from 0.8 to 0.83. Similarly, the controller is tested for voltage swell of 20% for a period of time  $t = 100\text{ms}$  and its corresponding output voltage and current through the linear load is checked. From Fig. 5c and 5d it is clear that the output (phase to neutral) voltages at PCC are controlled and maintained constant. The corresponding switching pulses are shown in Fig. 5e.

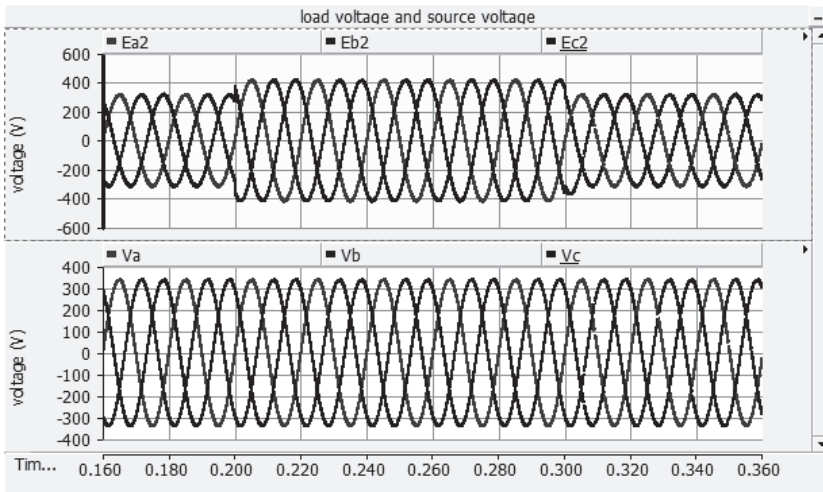


**Fig. 5c** – Waveforms of source voltages and Output (phase to neutral) voltages at PCC for voltage swell.

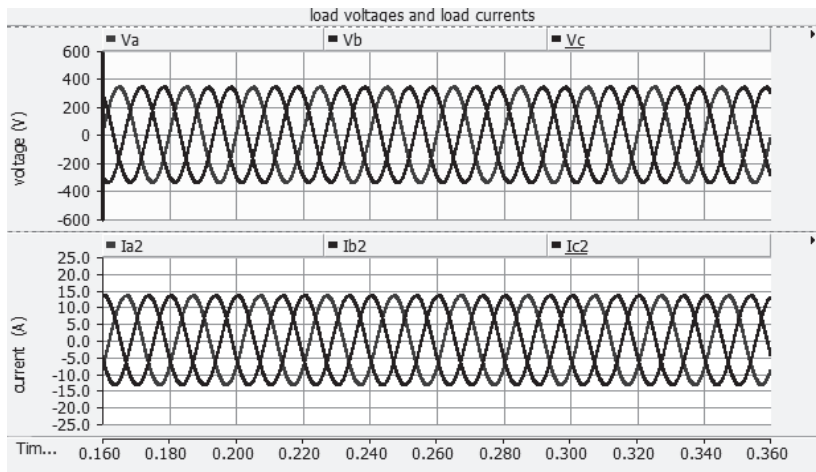


Fig. 5d – Waveforms of output voltages at PCC and load currents for voltage swell.

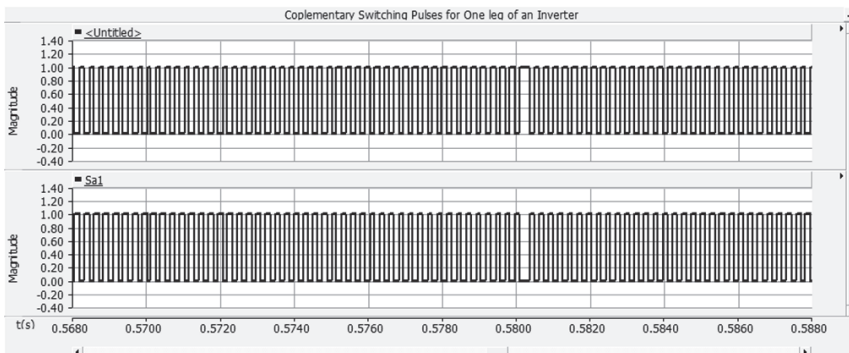


Fig. 5e – Complementary switching pulses for the switches in one leg of VSI.

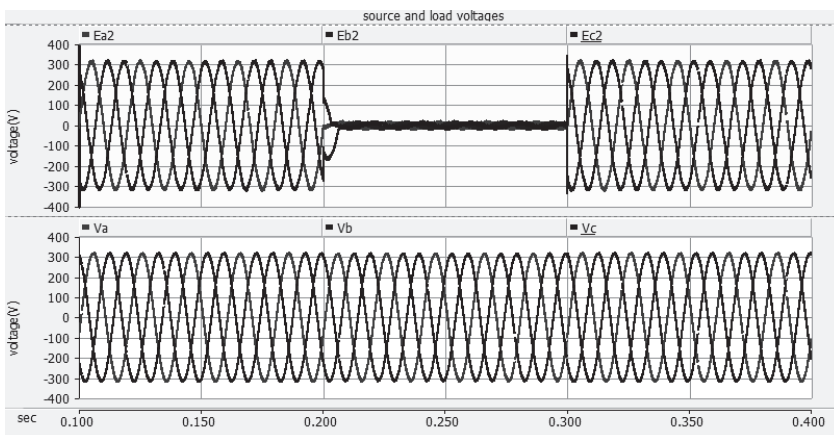
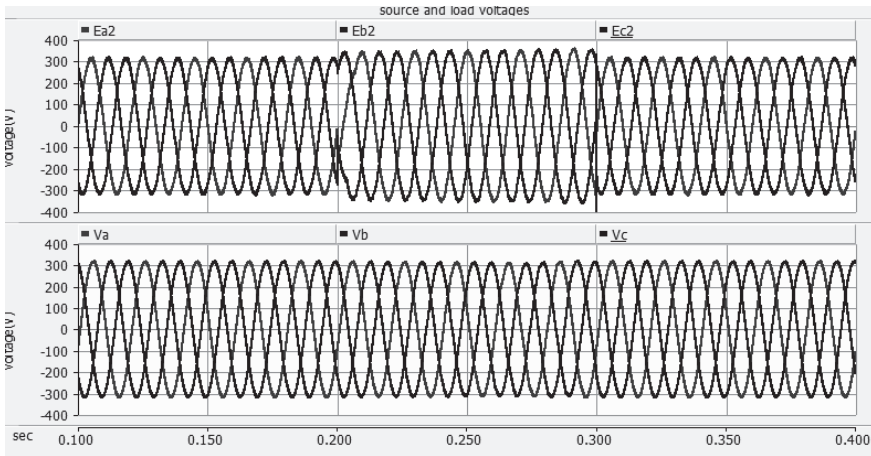


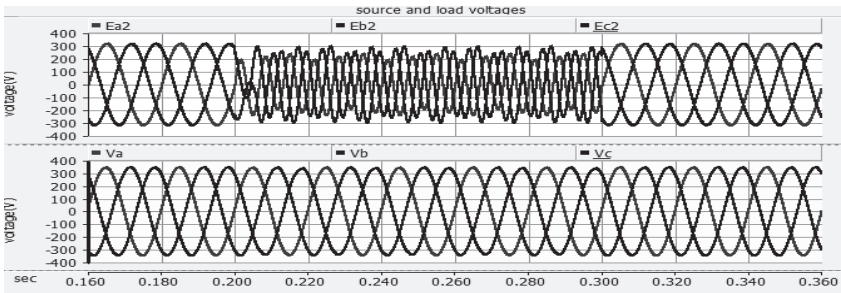
Fig. 5f – Source and load voltages for voltage interruptions of less than 10%.



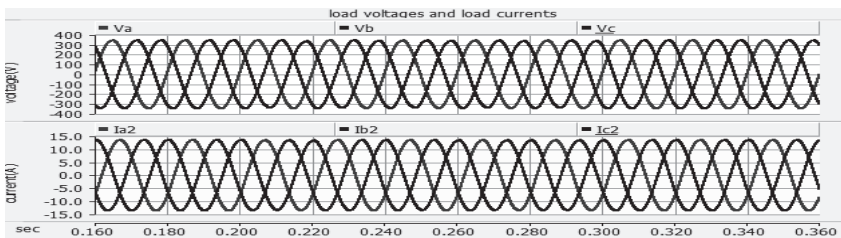
**Fig. 5g** – Source voltage and load voltage for a frequency deviation of 1 Hz.

### 3.2 Voltage harmonics and voltage unbalances

The designed Filter is tested by injecting the voltage harmonics along with the 20% voltage sag concurrently. These distortions are injected for a period of time  $t = 100$  ms. From Figs. 6a and 6b it is clear that the voltage at the load terminals is regulated and maintained as sinusoidal even though the voltage harmonics along with of 20% voltage sag is injected into the system.



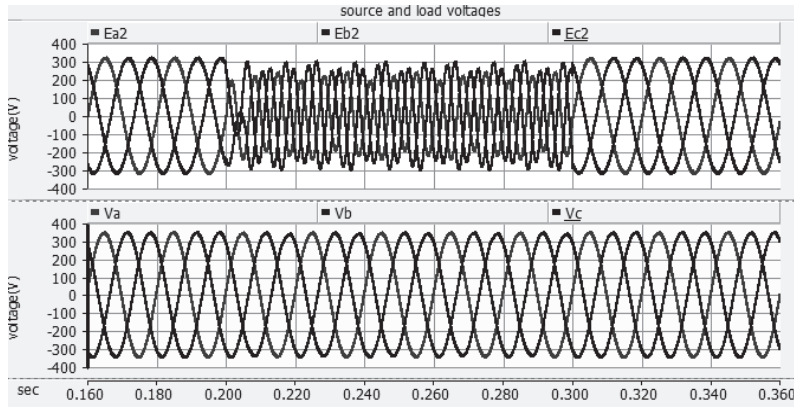
(a)



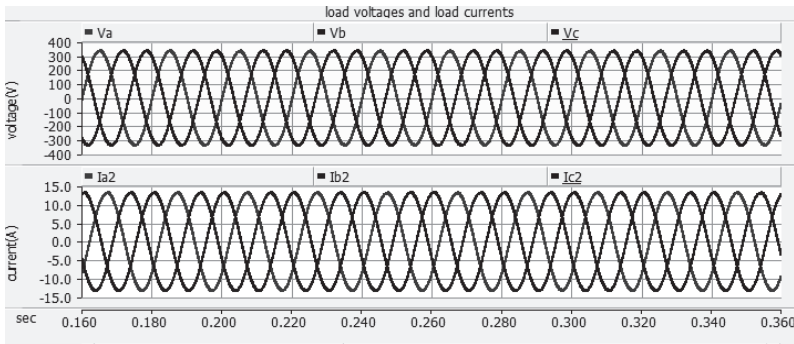
(b)

**Fig. 6** – (a) Waveforms of source voltages and output voltages at PCC; (b) Waveforms of output voltages at PCC and linear load currents.

Voltage unbalance is generated with voltage sag of 20% applied in one phase and voltage swell of 20% is applied in other two phases, the obtained source voltage and load voltage is as shown in the Fig. 7a. Voltage across the load and current through the linear load is as shown in Fig. 7b. From the waveforms obtained it is clear that the designed filter is removing the unwanted distortions present in the supply power and supplying the regulated power at the load terminals.



(a)



(b)

**Fig. 7** – (a) Waveforms of source voltages and load voltages;  
(b) Waveforms of load voltages and load currents.

The Total harmonic distortion present in line to line load voltages are in permissible limits as per the *IEEE-519* standard. Hence it can be concluded that the designed THSeAF is functioning effectively and supplying the regulated sinusoidal power to the linear loads by controlling the parameters from the load side. Load side SMC control leads to a stable system for any perturbations on the source side and is verified as per the Fig. 2a discussed in Section 2.

### 3.3 Load side SMC control in a three-phase system using P-Q theory

The voltage and current reference signals are generated by using the stationary reference frame and P-Q theory respectively. The block diagram of SMC using PQ theory is as shown in the Fig. 8. In the block diagram  $V_{aref}$ ,  $V_{bref}$ ,  $V_{cref}$  represents the reference voltages across the load and  $I_{caref}$ ,  $I_{cbref}$ ,  $I_{ccref}$  represents the reference voltages across shunt passive filter. The equations governing the PQ theory are given by (6) and (7),

$$P = V_{\alpha} I_{\alpha} + V_{\beta} I_{\beta} , \tag{6}$$

$$Q = V_{\beta} I_{\alpha} - V_{\alpha} I_{\beta} . \tag{7}$$

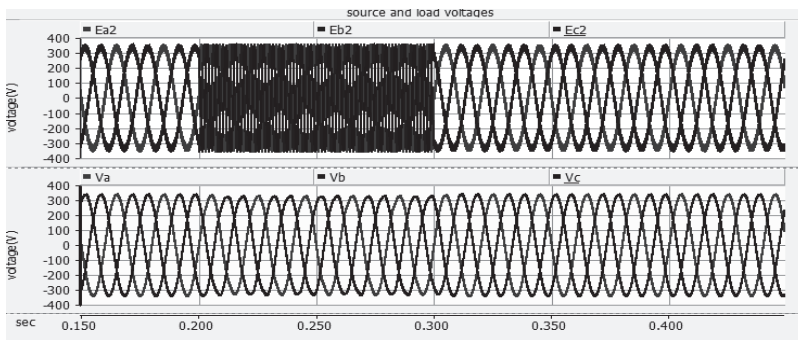
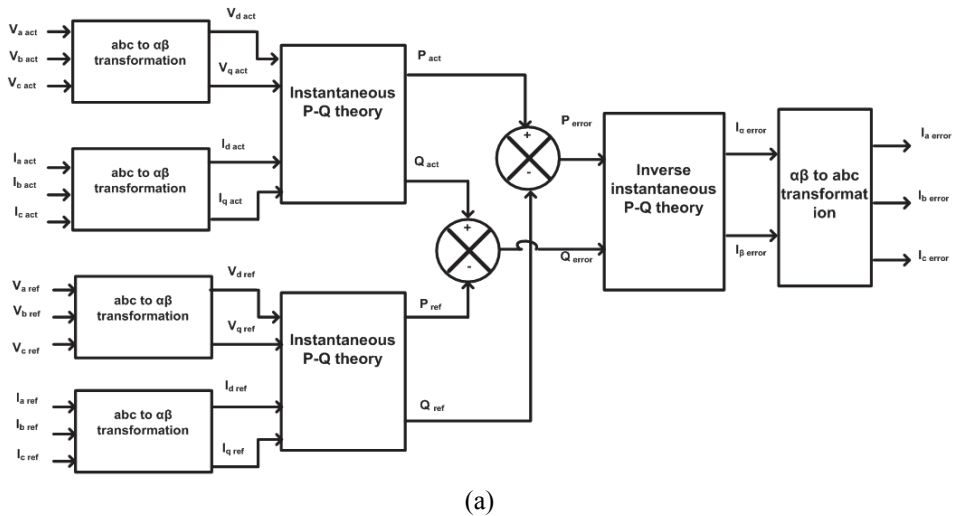


**Fig. 8** – (a) Block diagram representation of SMC for voltage and current reference generation using P-Q theory; (b) Simulation result for voltage harmonics compensation.

In this load side control the parameters from the load side i.e. voltage across the load  $V_L$  and current through the filter capacitor  $i_c$  is controlled. The reference signals for this voltage and currents are generated by using the stationary reference frame and P-Q theory equations. The reference actual three phase voltage and current signals are converted into the equivalent two phase signals by using the three phase to two phase transformations. The obtained two phase voltages and currents are given to the instantaneous P-Q block which will generates the  $P_{ref}$ ,  $Q_{ref}$  and  $P_{act}$ ,  $Q_{act}$ . Then by comparing the reference signals and actual signals the resultant  $P_{error}$  and  $Q_{error}$  are calculated. These errors are used to calculate the current error signals in two phase. These error signals are converted into three phase signals by using the three phase to two phase transformations.

From Fig. 8b it is clear that the load voltage is free of distortions irrespective of distortions in source voltage  $E_{a2}$ ,  $E_{b2}$  and  $E_{c2}$  respectively. It is observed during simulation in both PQ theory and stationary reference frame, if the voltage harmonics are injected along with voltage sag concurrently then the controller designed is unable to maintain the load voltage and current through the linear load as constant. This designed THSeAF is also observed to have low stability margins as discussed in Section 2. The controllable parameters are far away from the source. In real time there will be some amount of voltage drop due to the line impedance. Hence, it is quite difficult to make the system stable by controlling the load side parameters. Therefore, the focus has been shifted towards implementation of SMC by controlling supply side parameters.

#### 4 Source Side SMC Control

The frequency response characteristics are analysed by considering one of the phase in the three phase system which can be extended to the three phase system.

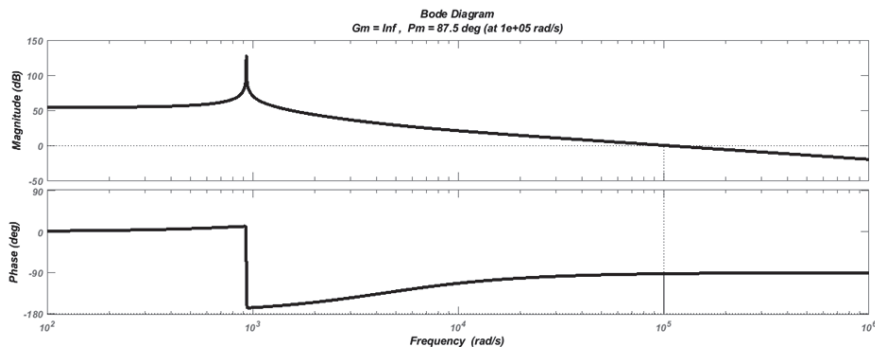


Fig. 9 – Open loop bode plot of THSeAF transfer function.

The state space variables chosen are voltage across the filter capacitor  $V_{cfi}$  and current through the filter inductor  $i_{se}$ . The stability of the system is analyzed by using the gain margins and phase margins obtained from the bode plot through state feedback approach. From Fig. 9 it is clear that the obtained system is stable with a gain margin of infinity and phase margin of 87.5 degrees. The block diagram representation of SMC for the source side control with sine wave generators is as shown in the Fig. 10.

In this case the voltage across the filter capacitor ( $V_{cfi}$ ) and current through the filter inductor ( $i_{se}$ ) are taken as an reference signals and are compared with the actual signals. Then the error signals obtained are multiplied by the sliding coefficients  $K_1$  and  $K_2$  then the resultant obtained error is given to the hysteresis logic to generate the firing pulses to the IGBT switches of H-Bridge Inverter.

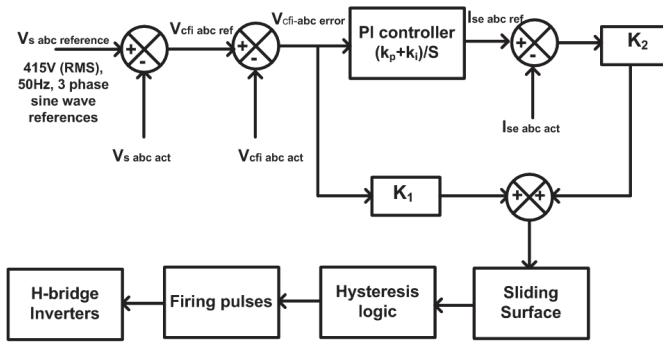


Fig. 10 – Block diagrammatic representation SMC for three phase systems source side control.

### 4.1.1 Simulation Results

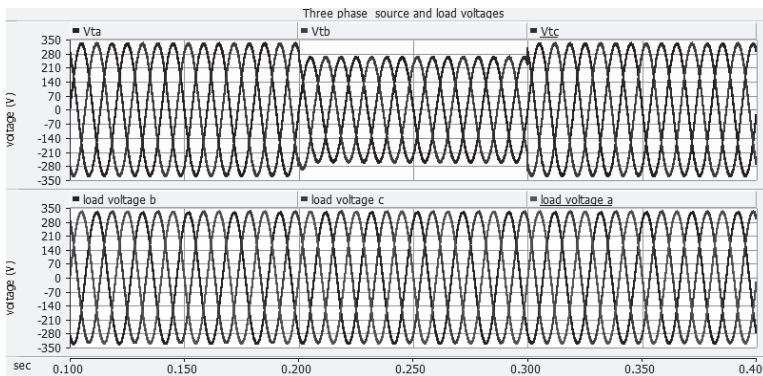
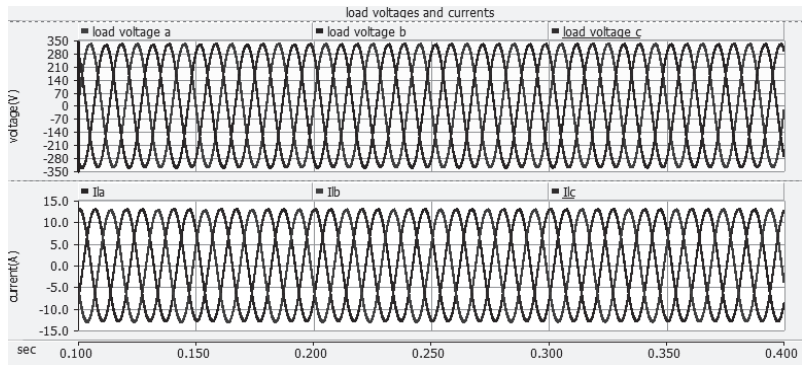
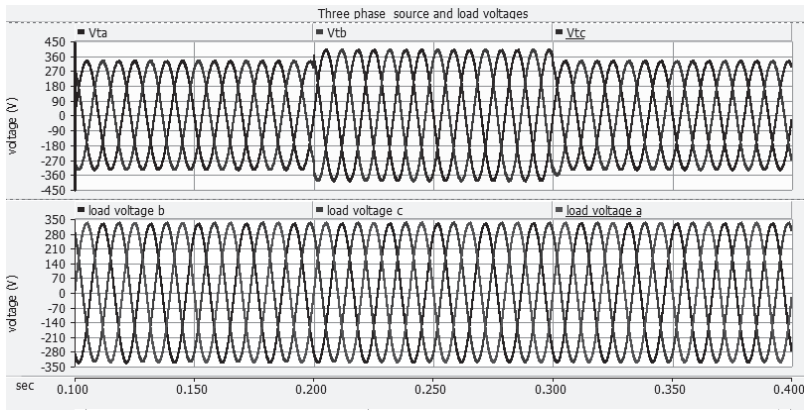


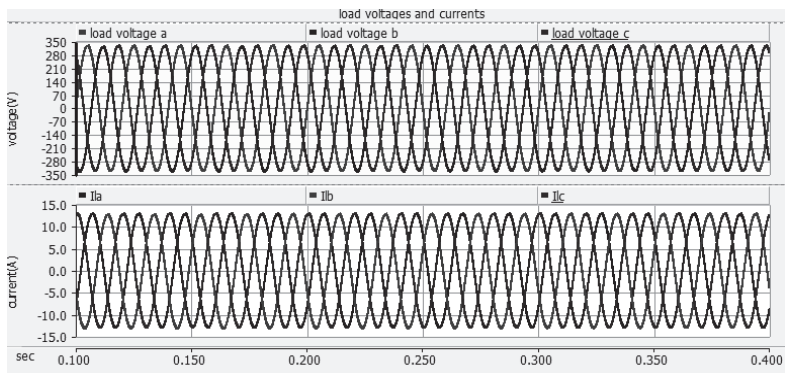
Fig. 11a – Waveforms of source voltages and linear load voltages.



**Fig. 11b** – Waveforms of linear load voltages and linear load currents.



(a)



(b)

**Fig. 12** – (a) Waveforms of source voltages and linear load voltages;  
(b) Waveforms of linear load voltages and linear load currents.



Fig. 11 and Fig. 12 show the simulation results obtained using sine wave generators as reference signals for sag and swell of 20%. The phase angle between the load voltage and load current is found to be 33.9 degrees.

It is clear that the load line to phase voltage of 240 V (rms) is maintained constant irrespective of the voltage sag and swell in the source voltage.

#### 4.1.2 Simulation Results of three phase system with source side control using stationary reference frame

The block diagram representation of SMC controller for voltage and current reference generation in the stationary reference frame is as shown in the Fig. 13a. In this circuit the reference signals and actual signals are generated in the stationary reference frame by using the three phase to two phase transformations. Then the corresponding error signals are generated by comparing the reference signal with the actual signal. The obtained error signals are then multiplied with the sliding coefficients and then given to the sliding surface. These signals are given to two phase to three phase transformation to generate the resultant error signal in each single phase of a three phase system. Thus the error signals generated from each phase is given to Hysterisis pulse width modulator to generate the firing pulses to the voltage source converter. Fig. 13b shows the corresponding load voltage and source voltage for a voltage sag of 20%. The designed THSeAF is analyzed for all the different voltage distortions and it can be concluded that the designed THSeAF injecting the voltage in phase and in out of phase against the distortions and maintains the regulated voltage at the load terminals. Hence by controlling the parameters from the source side constant desired voltage and current with less THD's is obtained compared to load side SMC control as given in **Table 2**.

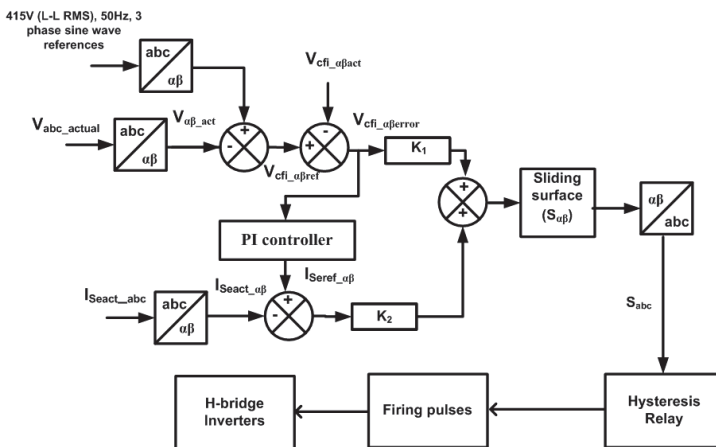
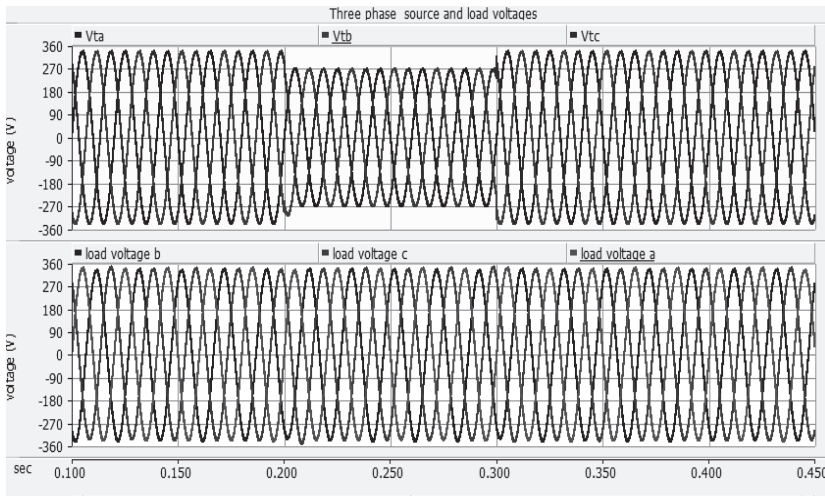


Fig. 13a – Block diagram representation of SMC for voltage reference and current reference generation in stationary reference frame for source side control.



**Fig. 13b** – Source and Load voltage for voltage sag for a duration of  $t=0.1s$ .

**Table 2** shows the obtained THD for various power disturbances when controlled using SMC at the source side and load side. It is realized that the results obtained are well within the IEEE standards.

**Table 2**  
*Percentage of THD's obtained for different power line disturbances.*

System	% of Voltage sag (THD in L-L voltages)	% of Voltage swell (THD in L-L voltages)	% of Voltage distortions (THD in L-L voltages)	% of Voltage unbalance (THD in L-L voltages)
Load side control (sine wave generators)	0.5 ,0.6, 0.9	0.5, 0.6 1.2	0.5, 0.6, 1.2	0.54, 0.6,1.2
Load side control (P-Q theory and stationary reference frame)	0.39, 0.38 ,0.38	0.32, 0.35, 0.35	0.3, 0.3, 0.3	----
Source side control (with sine wave generators)	0.48, 0.48, 0.48	0.482, 0.481, 0.481	0.48, 0.48, 0.48	0.48, 0.48 0.48
Source side control (stationary reference frame)	0.48, 0.48, 0.48	0.482, 0.481, 0.481	0.48, 0.48 0.48	0.48, 0.48, 0.48

**Table 3** shows the summary of the work carried out with load side and source side control for three phase system. The controller is robust and dynamic in obtaining the desired response within small duration of time.

**Table 3**

*Summary of SMC with load side and source side control three phase system.*

System	% Voltage (THD) range	Settling time (ms)	Shunt Capacitance required ( $\mu\text{F}$ )	% Current (THD) range
Three Phase (Load side control)	(0.3-1.3) L-L	7.5	228	0.59 – 0.62
Three Phase (Source side control)	(0.48-4.8) L-L	2.5	228	0.39 – 0.42

### 5 Short Circuit Protection Circuit

The designed THSeAF is connected directly to the system without the isolation transformer. Lack of short circuit protection to the THSeAF is a major concern. This THSeAF is connected in series to the supply. For example, if there is any short circuit fault like L-G fault on the load side then the load will draw the short circuit current from the source which will damage the designed THSeAF. In Fig. 14, two thyristors connected in anti-parallel work whenever there is a short circuit fault occurred on the load side thus protecting the device. The results are taken for a 120 V (rms), 60 Hz single phase system. The same type of protection can be extended for a three-phase system.

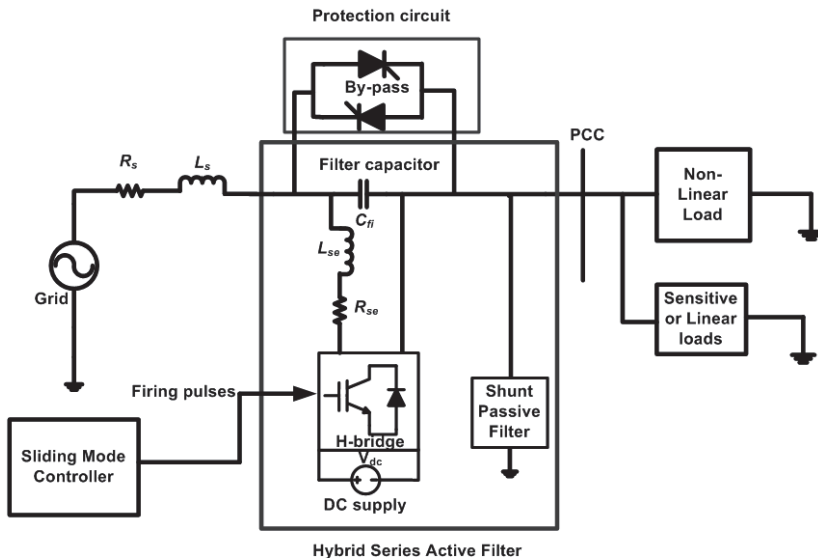
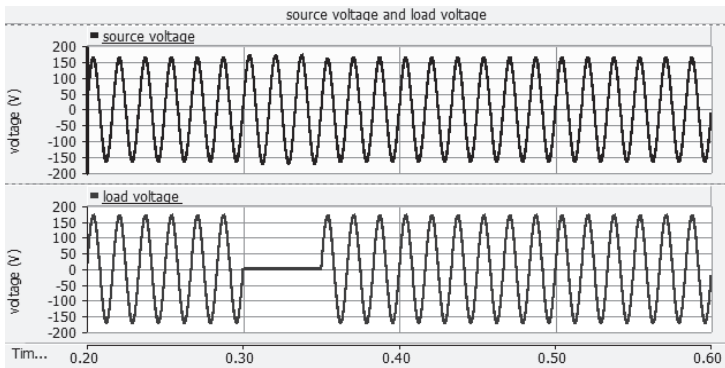
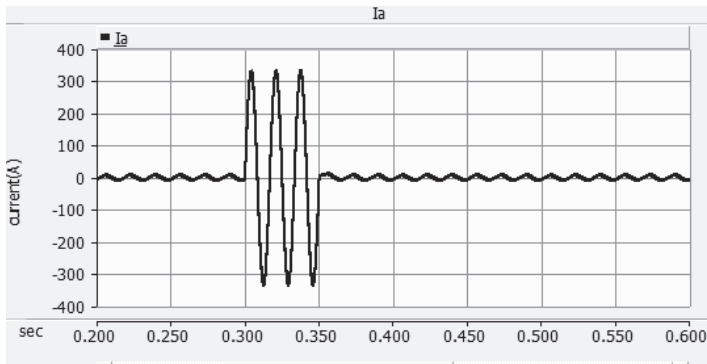


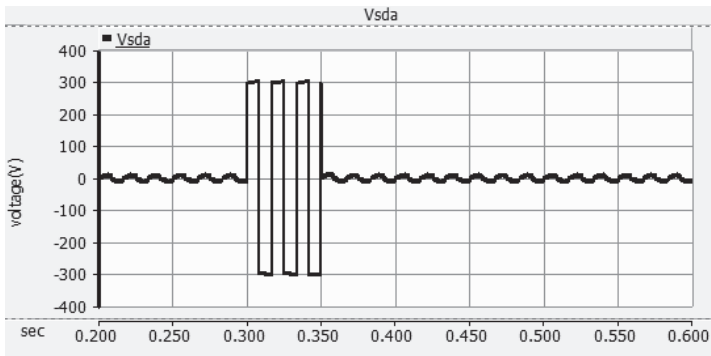
**Fig. 14** – Block diagram of short-circuit Protection circuit for THSeAF.



(a)



(b)



(c)

**Fig. 15** – (a) Waveforms of source voltage and voltage at PCC; (b) Waveform of source current; (c) Waveform of voltage across the Filter capacitor.

In this simulation the short circuit fault (L-G fault) has been created during the duration of time  $t = 0.3s$  to  $0.35s$ . Fig. 15a represents the waveforms of

source voltage and voltage at the load terminals. The voltage at the load terminals is found to be zero during the period of fault. Fig. 15b represents the waveform of source current. From the waveform it is clear that the load is drawing the short circuit current during the fault duration. Fig. 15c represents the waveform of voltage across the filter capacitor. During the duration of time  $t = 0.3\text{ s}$  to  $0.35\text{ s}$  the voltage across the filter capacitor is a square waveform which indicates the filter is isolated during the short circuit faults. Hence it is observed that the designed filter can be protected against short circuit faults using the circuit shown in Fig. 14.

## 6 Conclusions and Future Scope

The designed Transformerless Hybrid Series Active power Filter (THSeAF) is analysed in a three phase system by injecting the voltage distortions into the system. The control is done by considering the source side parameters as well as load side parameters. The mathematical modelling and stability analysis is presented which shows the system to possess good stability margins when SMC control is from source side. It is observed that it is unable to produce desired results when the two distortions are injected simultaneously using load side SMC control. The reference signals for currents and voltages are generated using instantaneous P-Q theory and stationary reference frame. The THD present in the output three phase line to line voltages is observed to be varying in the range of 0.3% to 1.2%. It is observed that the designed THSeAF works effectively in maintaining the load voltage constant. Less settling time of around 4 ms is observed during the operation. A short circuit protection circuit is proposed for protection of ThSeAF. The large short circuit current can be chopped by using the varistors across the short circuit protection circuit designed for THSeAF. The resultant short circuit current can be limited so that the loads are protected from the short circuit currents.

As part of future development, the readers can extend the work to a battery as an auxiliary supply for the proposed system using modular multi-level inverters.

## 7 References

- [1] A. Javadi, L. Woodward, K. Al-Haddad: Real-Time Implementation of a Three-Phase THSeAF Based on VSC and a P+R Controller to Improve Power Quality of Weak Distribution Systems, IEEE Transactions on Power Electronics, Vol. 33, No. 3, March 2018, pp. 2073 – 2082.
- [2] Power Electronic Handbook, Edited by M. H. Rashid, 3<sup>rd</sup> Edition, Elsevier Inc., Boston, USA, 2011.
- [3] Q.- N. Trinh, H.- H. Lee: Improvement of Unified Power Quality Conditioner Performance with Enhanced Resonant Control Strategy, IET Generation, Transmission & Distribution, Vol. 8, No. 12, December 2014, pp. 2114 – 2123.

- [4] A. Javadi, L. Woodward, K. Al-Haddad: An Advanced Control Algorithm for Series Hybrid Active Filter Adopting UPQC Behavior, Proceedings of the 38<sup>th</sup> Annual Conference on IEEE Industrial Electronics Society (IECON2012), Montreal, Canada, October 2012, pp. 5318 – 5323.
- [5] A. Javadi, K. Al-Haddad, S. Kouro: A Single-Phase Active Device for Power Quality Improvement of Electrified Transportation, IEEE Transactions on Industrial Electronics, Vol. 62, No. 5, May 2015, pp. 3033 – 3041.
- [6] A. Javadi, H. F. Blanchette, K. Al-Haddad: A Novel Transformerless Hybrid Series Active Filter, Proceedings of the 38<sup>th</sup> Annual Conference on IEEE Industrial Electronics Society (IECON2012), Montreal, Canada, October 2012, pp. 5312 – 5317.
- [7] A. Javadi, A. Hamadi, A. Ndtoungou, K. Al-Haddad: Power Quality Enhancement of Smart Households Using a Multilevel-THSeAF with a PR Controller, IEEE Transactions on Smart Grid., Vol. 8, No. 1, January 2017, pp. 465 – 474.
- [8] A. Ghosh, A. K. Jindal, A. Joshi: Design of a Capacitor – Supported Dynamic Voltage Restorer (DVR) for Unbalanced and Distorted Loads, IEEE Transactions on Power Delivery, Vol. 19, No. 1, January 2004, pp. 405 – 413.
- [9] A. F. Zobaa: Optimal Multiobjective Design of Hybrid Active Power Filters Considering a Distorted Environment, IEEE Transactions on Industrial Electronics, Vol. 61, No. 1, January 2014, pp. 107 – 114.
- [10] S. K. Gudey, R. Gupta: Sliding – Mode Control in Voltage Source Inverter-Based High-Order Circuits, International Journal of Electronics, Vol. 102, No. 4, 2015, pp. 668 – 689.
- [11] S. K. Gudey, R. Gupta: Sliding Mode Control of DVR for Mitigation of Source Side Voltage Disturbances, Proceedings of the IEEE International Conference on Standards for Smart Grid Ecosystem, Bangalore, India, March 2014.
- [12] S. K. Gudey, R. Gupta: Reduced State Feedback Sliding – Mode Current Control for Voltage Source Inverter-Based Higher Order Circuit, IET Power Electronics, Vol. 8, No. 8, August 2015, pp. 1367 – 1376.
- [13] A. Javadi, A. Hamadi, L. Woodward, K. Al-Haddad: Experimental Investigation on a Hybrid Series Active Power Compensator to Improve Power Quality of Typical Households, IEEE Transactions on Industrial Electronics, Vol. 63, No. 8, August 2016, pp. 4849 – 4859.
- [14] R. Gupta, A. Ghosh, A. Joshi: Performance Comparison of VSC – Based Shunt and Series Compensators Used for Load Voltage Control in Distribution Systems, IEEE Transactions on Power Delivery, Vol. 26, No. 1, January 2011, pp. 268 – 278.